Magnetopolaritons in a semiconductor quantum well microcavity

J. Tignon, R. Ferreira, J. Wainstain, C. Delalande, P. Voisin, and M. Voos
Laboratoire de Physique de la Matière Condensée de l'Ecole Normale Supérieure, 24 rue Lhomond, F 75005 Paris, France

R. Houdré, U. Oesterle, and R. P. Stanley
Institut de Micro- et Opto-éléctronique, Ecole Polytechnique Fédérale de Lausanne, CH 1015, Lausanne, Switzerland
(Received 30 January 1997; revised manuscript received 31 March 1997)

We present measurements of the vacuum Rabi splittings associated with the fundamental and the first three excited magnetoexcitons in a semiconductor microcavity up to 9 T. The oscillator strength values which are deduced from these experiments are compared to a simple and original variational calculation which includes the low magnetic-field (excitonlike) limit and the high magnetic-field (cyclotronlike) limit. Theoretical and experimental results are compared and discussed. [S0163-1829(97)05631-2]

The polariton concept has been known for a long time in semiconductor physics:[1] in a bulk material, the translation invariance of both the excitonic bound states and the electromagnetic modes induces the coupling of *one* excitonic state with *one* electromagnetic mode and thus the existence of mixed photon-exciton eigenstates named polaritons. The light-matter interaction is said to be in the strong-coupling regime. Because of the lack of translation invariance in the growth direction, this polariton concept disappears in two-dimensional quantum well (QW) structures unless a confinement of the electromagnetic mode exists in this direction. This is now realized by embedding the QW's in a wavelength-sized Fabry-Pérot-like structure of high finesse. The mirrors are composed of stacks of semiconductor Bragg mirrors grown in the same epitaxial run. The so-called vacuum Rabi splitting (VRS) resulting from the anticrossing of the photon mode and of the exciton mode has been observed in reflectivity measurements[2] and photoluminescence experiments.[3] Semiclassical or quantum theories[4,5] show that the VRS is a function of the finesse of the cavity, of the exciton oscillator strength f, and of the width of the excitonic line. In fact, a simple reflectivity or absorption experiment can give in microcavities a good measurement of the oscillator strengths, provided that the cavity and exciton linewidths are known. In particular, to observe a VRS of the so-called microcavity polaritons (MVP), the cavity and exciton mode widths must be small enough at a given f and, conversely, f must be large enough for given cavity and exciton mode widths.

This MCP concept is not relevant for the interaction of a confined electromagnetic mode with the *continuum* of unbound excitonic states at higher energy. In this case, the weak-coupling regime takes place. Nevertheless, Tignon *et al.*[6] have shown that, by quantizing this continuum of unbound states into discrete Landau levels, it is possible to observe new Rabi splittings at sufficiently large magnetic fields applied perpendicular to the QW structure. In fact, applying a magnetic field maintains the in-plane translational invariance and concentrates the oscillator strength into discrete magnetoexciton states. The oscillator strength increases with the magnetic-field value, and at given threshold fields, new VRS's occur. Only an estimate of these thresholds and of the VRS's was theoretically calculated, neglecting in particular the electron-hole interaction for excited Landau levels.[6,7] It was also shown in Ref. 6 (see also Refs. 8–10) that the Rabi splitting of the $1S$ exciton state increases with B, due to the magnetic-field-induced shrinkage of the $1S$ exciton wave function and to the subsequent increase of f. A quantitative agreement with a model using an exact calculation of the $1S$ exciton oscillator strength can be found in Ref. 8.

Three purposes are addressed in this paper. The first one concerns an improved measurement of the magnetic-field variation of the MCP modes related to QW magnetoexcitons up to the third excited one. The experiment is performed at 4.2 K up to 9 T. The MCP energies, in particular the values of the VRS's, are measured at a magnetic field larger than the threshold value where the Rabi splitting appears, and this for each magnetoexciton. Under the threshold, we show also that the variation of the reflectivity peaks reflects the variation of the electronic density-of-states between two magnetoexciton states. The second one provides an original variational calculation of the energy and of the oscillator strength of the fundamental and excited magnetoexcitons in the parabolic approximation. This calculation reproduces the low-field (essentially excitonlike) and large-field (essentially cyclotronlike) limits. As usual for a variational procedure, this approach provides a direct insight of the physical problem and can be reproduced without difficulty. The third purpose consists of a comparison between calculations and experiments of the magnetoexciton energies and, through a semiclassical treatment of the coupling between the electronic and the electromagnetic modes in microcavities,[4] of the Rabi splitting thresholds and of the oscillator strengths.

I. EXPERIMENTS

The sample, grown by molecular-beam epitaxy on top of a GaAs substrate, consists of a λ GaAs cavity embedded between two stacks of distributed Bragg layers: the top (bottom) mirror contains 15 (19.5) pairs of AlAs and GaAs λ/4 mirrors. In the middle of the λ cavity, where an antinode of the electric field occurs, three 75-Å-thick $In_{0.13}Ga_{0.87}As$

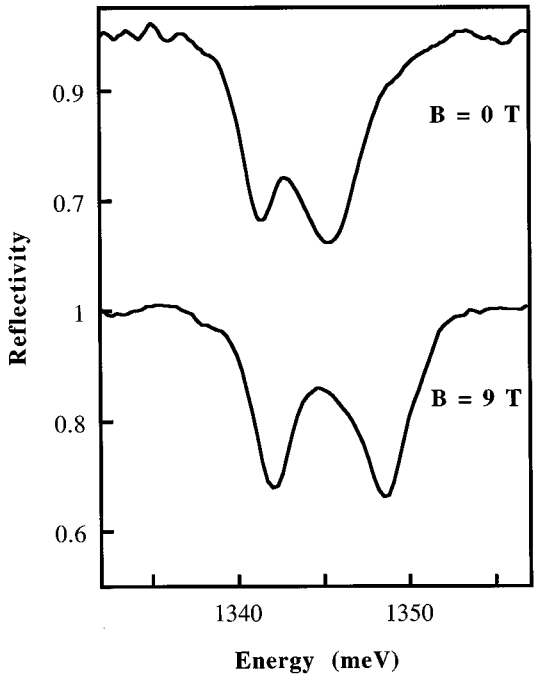

FIG. 1. Reflectivity spectra of the microcavity at $B=0$ and 9 T at spot locations where the optical mode is in resonance with the $1S$ exciton state. For clarity the two curves are shifted one from each other.

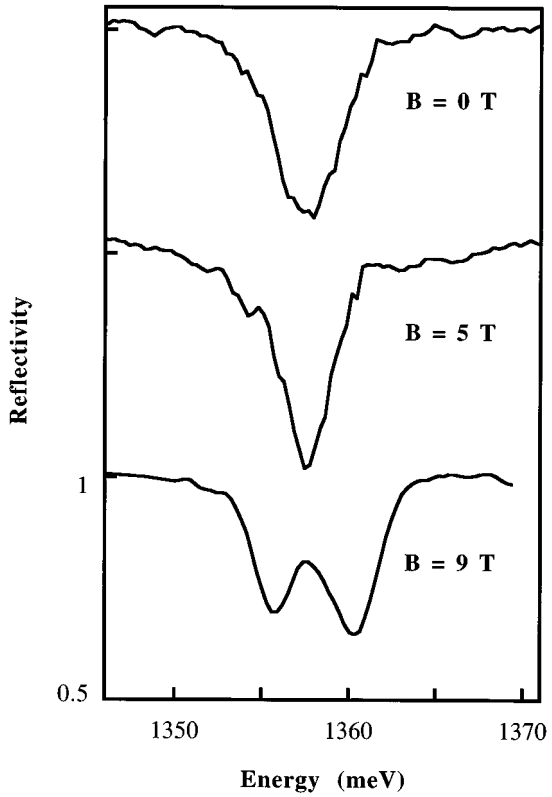

FIG. 2. Reflectivity spectra of the microcavity at a spot location where the cavity mode energy is 1358 meV. At $B=0$ T, the cavity mode is in resonance with the continuum of excitonic states. At $B=5$ T, the width of the reflectivity peak is smaller than at vanishing B. At $B=9$ T, this cavity mode is in resonance with the first excited magnetoexciton level, with a coupling strong enough to observe the VRS.

QW's, separated by 100-Å-thick GaAs barriers, are grown. An interruption of the rotation of the sampling during growth provides a tunability of the cavity mode energy (E_{cav}) under normal incidence with respect to the $1S$ exciton energy (E_{exc}) at vanishing B across the wafer. After suitable characterization of the sample by low-temperature photoluminescence and reflectivity experiments, which allows an experimental determination of E_{cav} and E_{exc}, the sample was introduced in a superconducting magnet which provides fields up to 9 T. The temperature was 4.2 K. A tunable Ar^{+}-pumped Ti:sapphire laser was focused on the sample by a $f=1$ m lens. In the geometry used in the experiment, it was calculated and checked experimentally that the laser waist diameter was 250 μm, which prevents any broadening of the lines due to the cavity and exciton energy variations across the wafer and to the angular dependence of the cavity mode. The reflectivity was collected using a semireflecting plate and focused on an optical fiber, before analysis by an $In_xGa_{1-x}As$ photomultiplier through a monochromator which follows the wavelength variations of the tunable laser.

By choosing the spot location on the sample, it is possible to find the resonance between the cavity mode and the $1S$ exciton mode and to observe, at $B=0$, the related VRS (Fig. 1, top). A small modification of the spot location allows us to follow the resonance between the cavity mode energy and the exciton mode energy shifted by the diamagnetic effect. An increase of the Rabi splitting Ω_0 (Fig. 1, bottom) is observed,[6,8,10] from 3.7 up to 6.5 meV at 9 T. Also observed in Fig. 1 is the symmetrization of the width of the reflectivity lines as the field is increased. At low magnetic field, the high-energy polariton line is broader than the low-energy polariton line. This behavior disappears at large B. The small asymmetry in the reflectivity peaks, which appears in some of the spectra presented in Figs. 1 and 2, *is* due to a nonperfect resonance point location, but the values of the energies of the MCP modes at resonance reported in this paper are not affected by this small uncertainty.

At another spot location, where the cavity mode is in resonance with the continuum of excitonic states, no VRS is observed in the reflectivity experiment (Fig. 2, top), as the electromagnetic mode is, in this case, in interaction with a continuum of electronic states. The width of the reflectivity mode (3.5 meV) is larger than the width of the cavity mode measured at a sample point where all the layers are transparent (1 meV). This is due to the absorption by the continuum of QW states which reduces the cavity finesse. With increasing B, the reflectivity peak width shows small variations, as seen later, before the observation of a VRS at a given field (Fig. 2, bottom). By mapping the sample surface, it is possible to measure the MCP mode energies as a function of B. This is shown in Fig. 3 (symbols). Apart from the $1S$ exciton MCP doublet, up to three excited doublets Ω_1, Ω_2, and Ω_3 appear. With respect to previous publications,[6,11] the number of exciting spots and of B values has been considerably increased. It enables us to show clearly that the critical B value for which a new excited VRS appears increases with the excited state index: 3.25, 4.5, and 7.6 T. Figure 4 reproduces the four magnetic-field variations of the VRS's when they exist.

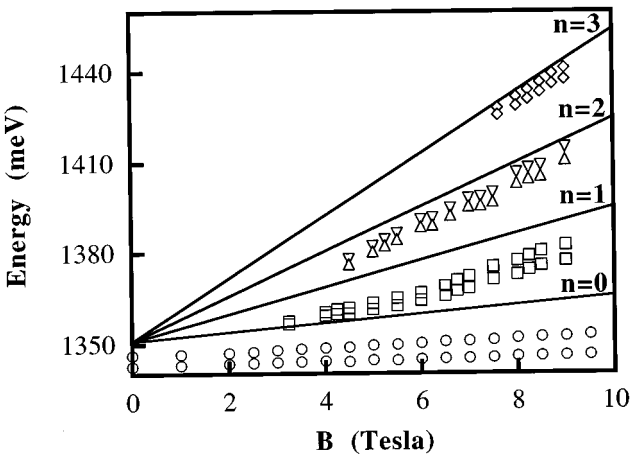

FIG. 3. (Solid lines) Calculated transition energies between electron and hole Landau levels using the parameters given in the text and neglecting the excitonic effect. The various symbols represent the energies of the reflectivity doublets when a VRS is observed.

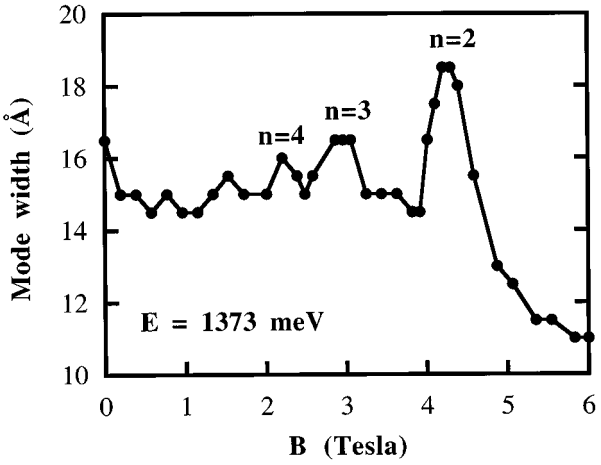

FIG. 5. Width of the reflectivity peak as function of B at a spot location where the cavity mode energy is 1373 meV. At this point, a VRS related to the first excited Landau transition appears at 8 T. The solid line is a guide to the eye.

In the first approximation, the mean energy of the doublets is compared to the energies of the transitions which involve Landau electron and heavy-hole states (solid lines in Fig. 3): $E_n=(n+\frac{1}{2})\hbar eB(1/m_e+1/m_h)$, with $m_e=0.07m_0$ and $m_h=0.09m_0$ are the electron and in-plane heavy-hole masses.[12] The strain occurring in the $In_xGa_{1-x}As$ QW's due to the lattice mismatch, which pushes the light-hole level 70 meV away from the heavy-hole level, allows the use of a simple parabolic mass for the holes. Obviously, the agreement is not very good, not only for the fundamental transition, where it is well known that the excitonic effect is predominant, but, to a lesser and lesser extent, for the excited transitions. The electron-hole correlation must not be neglected: excited magnetoexcitons are involved.

Another proof of the electron-hole correlation importance is the existence of B thresholds for the observation of new VRS's which increase with the Landau-level index. Without electron-hole correlation, the oscillator strength of a 2D Landau level increases proportionally to B, like the Landau-level degeneracy, and is independent of the Landau-level index. For given cavity mode and electronic mode widths, these thresholds might be independent of the level index. Experimentally, this is not the case, which shows the necessity of taking into account the exciton effect, even for excited magnetoexcitons, in contrast to what was done in previous publications.[6,11] The fact that the threshold value increases with the index level indicates that the electron-hole correlation is less and less important. This shows also that the investigation of the VRS's provides a good tool for measuring the oscillator strengths of magnetoexcitons.

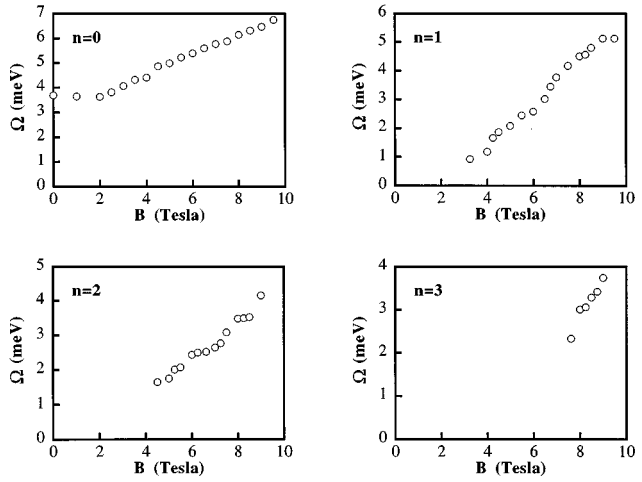

FIG. 4. Measured VRS as a function of B for the fundamental ($n=0$) and the three first excited transitions ($n=1-3$).

Before comparing theory and experiment, we present in Fig. 5 the variation with B of the width of the reflectivity peak below the Rabi splitting threshold (at the energy chosen in Fig. 5, a Rabi splitting occurs near 8 T for the $n=1$ magnetoexciton). In this range of B, the weak-coupling description is relevant and these oscillations in the width are the consequence of variations of the absorption coefficients, which themselves depend on the energy-dependent density of states. The width maxima occur when a magnetoexciton state is resonant with the cavity energy, which gives another measurement of the energies of the magnetoexcitons even under the strong-coupling threshold. The minima give, within a precision which depends essentially on the electronic mode width (measured to be 5 meV in this sample), the residual density of states between two Landau levels. It is worth noticing that the microcavity, as a result of the multiple reflections on the Fabry-Pérot mirrors, allows an easy measurement of the absorption coefficient without multiplying the number of QW's.

II. CALCULATION OF THE MAGNETOEXCITON STATES

We use a variational procedure to calculate the magnetoexciton states in a quantum well. Among the methods proposed in the literature to theoretically handle the magnetoexciton problem we quote the diagonalization of the envelope Hamiltonian in a Gaussian basis,[13] the exact numerical inte-

gration of the Schrödinger equation,[8] and the two-point Padé approximant method of MacDonald and Ritchie.[14] We discuss now an original variational proposition to describe the magnetoexciton states in quantum wells.

Firstly, we use the fact that in our sample with three decoupled strained $In_{0.13}Ga_{0.87}As$-GaAs quantum wells the fundamental light and heavy holes are well separated in energy ($\approx$70 meV) in order to safely neglect the hole-band mixings.[15] Secondly, we assume a decoupling of the in-plane and confined (along the growth axis and B direction) motions (a good assumption for excitons if the well width is not too large).[16] Third, we take advantage of the fact that the fundamental electron [energy $E1$ and envelope $\phi_1(z_e)$] and hole [energy H_1 and envelope $\chi_1(z_h)$] levels are well separated in energy from higher confined levels, and assume that the zero-field exciton levels are solutions of an effective two-dimensional potential, $V_{\rm eff}(\rho)$, obtained by averaging the three-dimensional Coulombic one over the confined electron and hole z motions:

$$V_{\rm eff}(\rho)=(-e^2/\kappa)\int\int dz_e dz_h[\phi_1(z_e)\chi_1(z_h)]^2/[\rho^2+(z_e-z_h)]^{1/2}, \tag{1}$$

where κ is the dielectric permeability and ρ the electron-hole distance in the plane of the layers. Finally, by properly choosing the field gauge we have the well-known ($K=0$) exciton Hamiltonian[16]

$$H_{\rm exc}(\rho)=T_\rho+V_{\rm eff}(\rho)+(\mu/2)(\omega_c/2)^2\rho^2, \tag{2}$$

where the first term is the kinetic energy and the last one is the magnetic-field contribution. We take for the ground, $1S$-like exciton state the form

$$\Phi_{1S}(\rho)=N_{1S}\exp\{-(\rho/\lambda_{1S})^{\alpha_{1S}}\}, \tag{3}$$

where λ_{1S} and α_{1S} are B-dependent variational parameters and N_{1S} the normalization constant. This envelope is expected to be flexible enough to smoothly interpolate between the $\alpha_{1S}\approx 1$ value at weak fields (when $B=0$, the $\alpha_{1S}=1$ value gives the exact result for the two dimensional case and is often used as a trial for excitons in actual quantum wells[16]) and the $\alpha_{1S}\approx 2$ value at very high fields. In principle, the numerical methods in Refs. 8 and 13 for actual QW's can provide the exact solution for the magnetoexciton problem, even though, in the general case, a heavier computational work, which does not bring any new insight into the physics involved in such investigations, is needed to provide highly accurate results. A variational procedure, on the other hand, permits a more physical approach to the problem. In addition, we have checked that our variational function for the ground state reproduces with high accuracy the corresponding results of MacDonald and Ritchie[14] for the two dimensional case and those of Fisher *et al.*,[8] for an actual quantum well. A further advantage of our approach is that the variational procedure can be easily generalized to the excited-exciton states. The variational envelope for the nS-like state reads

$$\Phi_{nS}(\rho)=N_{nS}P_{nS}[\rho/\lambda_{1S}]\exp\{-(\rho/\lambda_{nS})^{\alpha_{nS}}\}, \tag{4a}$$

$$P_{nS}[X]=\sum_{k=0,n-1}A_{nS,k}(X)^{k\alpha_{nS}}, \tag{4b}$$

where $A_{nS,0}=1$ and the remaining $n-1$ coefficients $A_{nS,k}$ are determined by orthogonalization with the $n'S$ envelopes: $\langle\Phi_{n'S}(\rho)|\Phi_{nS}(\rho)\rangle=0$ with $n'=1,2,\ldots,n-1$. Finally, λ_{nS} and α_{nS} are the only B-dependent variation parameters and N_{nS} the normalization constant. Exciton series with different angular dependences can be generated in a similar way. These, however, are not considered in this work since they correspond to optically inactive states.

Another parameter of interest is the exciton oscillator strength. According to Eq. (4) it is proportional to the square of the normalization constant. We define correspondingly $O_{nS}(B)=|N_{nS}(B)|^2$ for the nS-like level.

The solid lines in Fig. 6 are the calculated energies for the first four nS-like magnetoexcitons [$n=1-4$ in Eqs. (3)] in our structure. Note for a fixed n value the passage from a roughly quadratic variation at weak fields (diamagnetic shift) to a quasilinear (Landaulike) behavior at large fields. This passage occurs around a magnetic-field $(B_c)_{nS}$ value which decreases with increasing n. Correspondingly (Figs. 7 and 8), the variational parameters λ_{nS} and α_{nS} also present an important variation with the field around $(B_c)_{nS}$, and the transition towards the high-field values ($\alpha_{nS}\approx 2$ and λ_{nS}

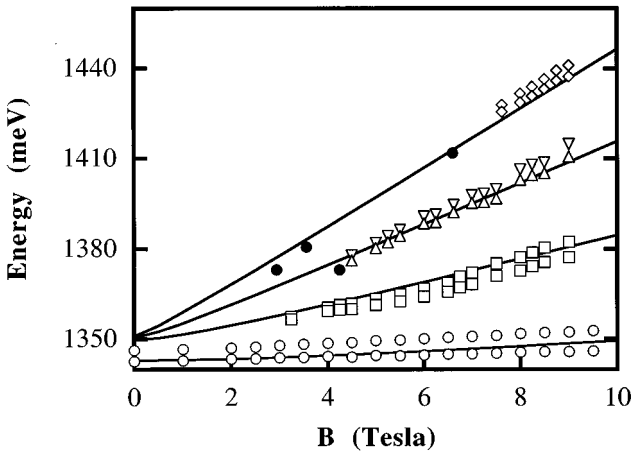

FIG. 6. (Solid lines) Calculated magnetoexciton transitions following the variational procedure explained in the text. The solid circles represent some of the experimental points deduced from the maxima of the reflectivity width in the weak coupling regime (Fig. 5) which indicate the magnetoexciton transition energies. The other symbols reproduce the experimental energies of the reflectivity peaks above the threshold.

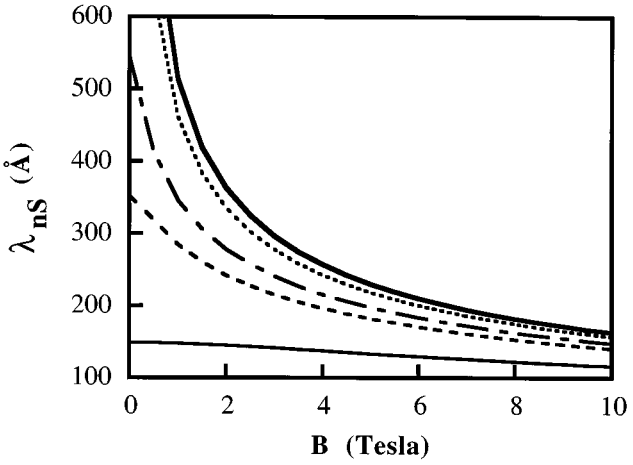

FIG. 7. Magnetoexciton radii resulting from the variational procedure for the nS excitons. For a fixed B value there is $\lambda_{1S}<\lambda_{2S}<\lambda_{3S}<\lambda_{4S}<\lambda_c$, λ_c being the cyclotron radius calculated without taking into account the electron-hole interaction. Note that the nS exciton is associated with the $(n-1)$th Landau transition.

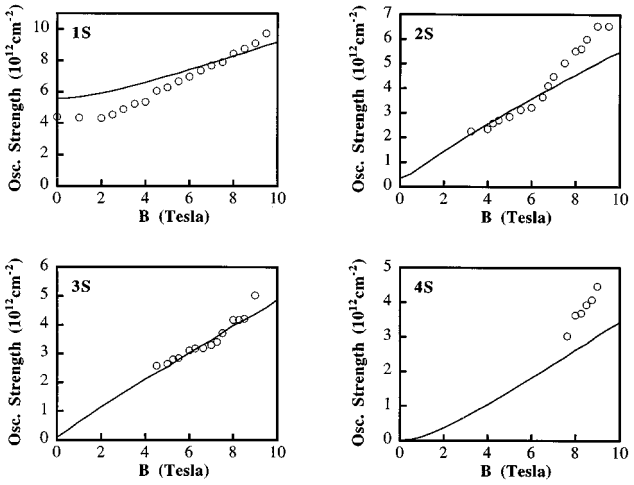

FIG. 9. Variation with the magnetic field of the oscillator strength of the magnetoexcitons. The solid lines are the result of the variational procedure. The circles are deduced from experiment.

$\approx\lambda_c$ is the cyclotron radius) is the steepest for the excited levels (with increasing n). The evaluated $OS_{nS}(B)$ (solid lines in Fig. 9) increase with B and show a roughly linear dependence at high fields, as expected (at high fields the extension of the in-plane wave functions decreases like the cyclotron radius $\lambda_c\approx B^{-1/2}$, which gives $OS\approx 1/\lambda_c^2\approx B$).

III. COMPARISON BETWEEN THEORY AND EXPERIMENT

The first comparison concerns the energies of the magnetoexciton transitions. The good agreement between calculated and measured values is shown in Fig. 6. Even the small discrepancy occurring for the $n=3$ level can be explained by the simplifying use of $\alpha=2$ for the theoretical calculation in this particular case: the magnetoexciton binding energy is then underestimated and the calculated transitions are actually found above the experimental ones. The solid circles in Fig. 6 represent some of the experimental points deduced from the maxima of the reflectivity width in the weak-coupling regime (Fig. 5), which indicate the magnetoexciton transition energies.

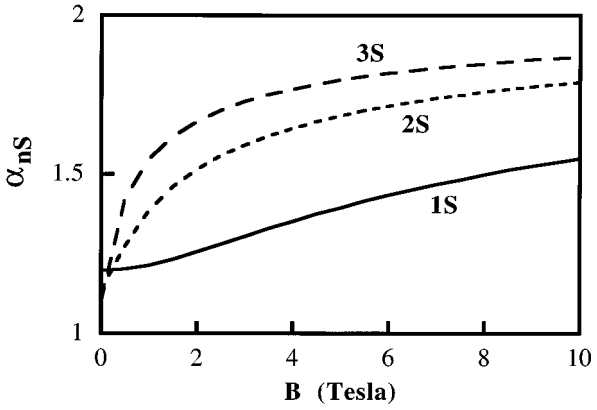

FIG. 8. Parameter α_{nS} resulting from the variational procedure for the nS excitons. The high-field cyclotron limit corresponds to $\alpha\approx 2$ and the low-field exciton limit corresponds to $\alpha\approx 1$.

The comparison between theory and experiments for the oscillator strengths requires a modelization of the photon-magnetoexciton coupling in the strong-coupling limit. As it is now well established,[5] quantum and semiclassical treatments give essentially the same results. We use here the adaptation,[4] relevant for semiconductor microcavities, of the semiclassical model[17] relevant for atomic physics. The reflection and transmission properties of the electromagnetic wave are treated by standard transfer-matrix methods whereas the absorption and dispersion of the discrete excitonic states are introduced through a Lorentzian-shaped energy-dependent dielectric constant. The width of the electromagnetic mode is calculated and measured experimentally by reflectivity measurements under the $1S$ QW resonance. The width of the excitonic mode, which is found in this sample essentially independent of B and of the level index, is deduced from the width of the MCP modes at resonance: in this model where the line is assumed to be *homogeneous*, the width of the MCP mode at resonance is the average value of the photon and electron modes. With this procedure, we find 5 meV for the exciton mode width. Note that the Zeeman splitting of the magnetoexciton, which is of the order of 1 meV at 9 T,[8] is neglected here with respect to the excitonic mode width. These parameters are therefore deduced from our experimental results and the last input parameter in this model is thus f, the oscillator strength per unit area of one QW. Conversely, the Rabi splitting value gives the f value.

The result of the model calculation as a function of the unknown f is shown in Fig. 10 both for a low-width electronic state and for the actual values in our sample. Note that the $\Omega\propto\sqrt{f}$ behavior is valid only for Rabi splittings Ω large with respect to various linewidths and that in our case the threshold value of f is 2×10^{12} cm^{-2}. We take this f value for the $n=1$ magnetoexciton at $B=3.25$ T (the threshold for the $n=1$ magnetoexciton) as the fit parameter to compare the relative values of the calculated OS and the measured (through the above model) f for all the magnetoexcitons at

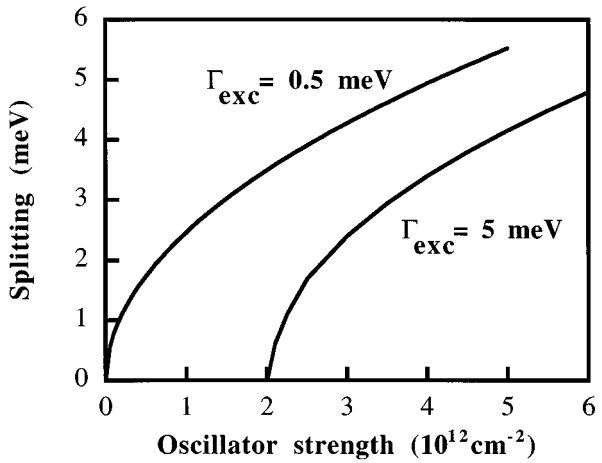

FIG. 10. Calculated VRS as a function of the oscillator strength for two exciton mode widths. The photon mode width is 1 meV.

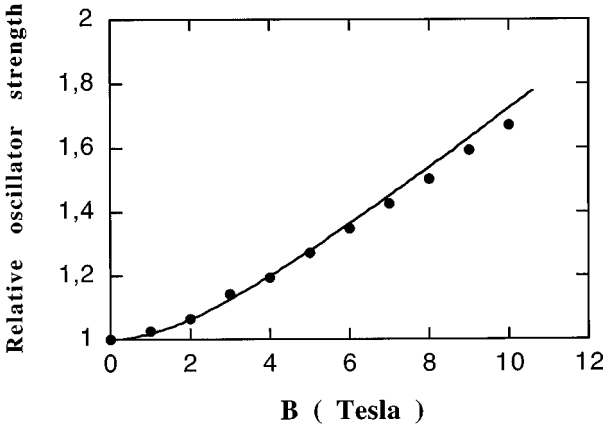

FIG. 12. Relative magnetic-field variation of the 1*S* exciton oscillator strength calculated by our variational method (solid curve), compared to the method of Ref. 8, in the case of the sample of Ref. 8. The solid circles reproduce some calculated values taken from Ref. 8.

all magnetic fields. Figure 11 compares first the calculated (circles) and measured (crosses) *B* thresholds for the excited magnetoexcitons. The agreement between theory and experiment is excellent. This tends to show that the relative oscillator strengths of the magnetoexcitons are well given by the simple variational calculation. But the agreement is not as good, although quite reasonable, if one compares the magnetic-field variation of the oscillator strengths for the various magnetoexcitons (Fig. 9). In most cases, the *f* experimental variation seems larger than the calculated one, in particular for the 1*S* exciton line.

The validity of the variational calculation could be questioned first. But we have checked that, when applied to the sample of Fisher *et al.*,[8] our variational method gives the same variation with the field for the 1*S*-state oscillator strength as the one reported in Ref. 8, obtained by the exact solution of the Schrödinger equation. The comparison is shown in Fig. 12. Our opinion is that the small discrepancy between theory and experiment is mainly due to the *inhomogeneous* nature of the exciton line. Indeed, we have performed a lot of simulations which considered for the excitonic mode: (1) a homogeneous (Lorentzian shape) broadening with a homogeneous mode width varied from 0.1 to 1 meV, and (2) an inhomogeneous (Gaussian shape) broadening with a mode width of 5 meV. The reflectivity spectrum in these cases was calculated to be the superposition (with the same Gaussian weight) of the reflectivity spectra of homogeneously broadened lines. The results of this simulation do not modify essentially the *f* values obtained here. Furthermore, it was impossible in our case to promote one of the existing theories of the inhomogeneous broadening of microcavity polaritons: (i) Rabi splittings not modified by the inhomogeneous broadening and MCP mode widths related to the homogeneous width of the QW state,[18] or (ii) the effect of the motional narrowing on the width of the MCP lines related to the very small in-plane mass of the MCP modes at resonance.[19] Note that both theories assume that the Rabi splitting is large enough with respect to the mode widths. We are not in this regime here, in contrast to the 1*S*-like state in the sample of Ref. 19, and it will never be possible to be in this regime near the thresholds for the excited magnetoexcitons. Other theories and systematic studies on different samples are necessary to solve this problem.

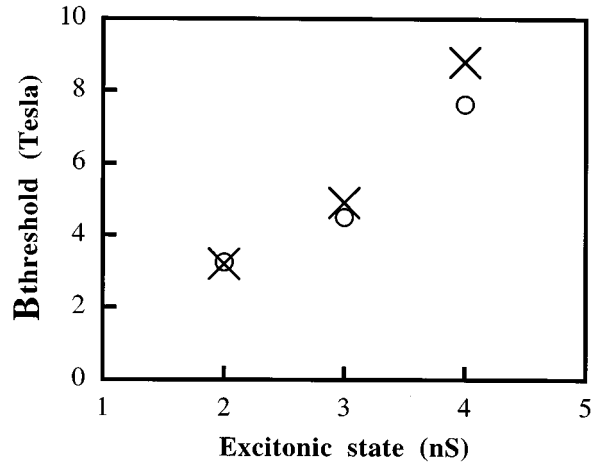

FIG. 11. Calculated *B* thresholds (crosses) for the excited magnetoexcitons compared to the experimental ones (circles). The fit parameter is adjusted to get a good agreement for the 2*S* magnetoexciton threshold.

IV. CONCLUSION

In conclusion, we have systematically measured the magnetic-field variation of the Rabi splittings in a QW semiconductor microcavity. Up to four Rabi splittings have been observed at 9 T. The thresholds for which the oscillator strength of the excited transitions is large enough for the observation of the strong coupling behavior have been determined. We have evidenced the fundamental role of the electron-hole interaction, even for the excited Landau transitions. We took advantage of a strained-induced simple parabolic hole dispersion relation to propose a variational calculation of the energies and of the oscillator strengths of magnetoexcitons in QW's. This calculation gives the good values in the low-field (excitonlike) and high-field (Landau-

level-like) limits. The Rabi splitting measurements gave us the opportunity to measure the oscillator strength. The agreement between theory and experiment is quite good for the overall results with only one fit parameter. The remaining discrepancies are most likely related to the inhomogeneous nature of the QW's linewidths for which a treatment of the strong-coupling behavior near threshold is necessary.

ACKNOWLEDGMENTS

The Laboratoire de Physique de la Matière Condensée de l'Ecole Normale Supérieure is Laboratoire Associé aux Universités Paris 6, Paris 7 et au CNRS. The work at Ecole Polytechnique Fédérale de Lausanne was partly supported by Thomson CSF, the Swiss National Program for Optics and the Esprit Smiles Program.

[1] For a review, see, for instance, C. Weisbuch and R. G. Ulbrich, in *Light Scattering in Solids III*, edited by M. Cardona and G. Günterodt, Topics in Applied Physics (Springer, Berlin, 1982), Vol. 51.

[2] C. Weisbuch, M. Nishioka, A. Ishikawa, and Y. Arakawa, Phys. Rev. Lett. **69**, 3314 (1992).

[3] R. Houdré, C. Weisbuch, R. P. Stanley, U. Oesterle, P. Pellandini, and M. Ilegems, Phys. Rev. Lett. **73**, 2043 (1994).

[4] R. Houdré, R. P. Stanley, U. Oesterle, M. Ilegems, and C. Weisbuch, Phys. Rev. B **49**, 16 761 (1994).

[5] V. Savona, L. C. Andreani, P. Schwendimann, and A. Quattropani, Solid State Commun. **93**, 733 (1995).

[6] J. Tignon, P. Voisin, C. Delalande, M. Voos, R. Houdré, U. Oesterle, and R. P. Stanley, Phys. Rev. Lett. **74**, 3967 (1995).

[7] S. Jorda, Solid State Commun. **97**, 7 (1996).

[8] T. A. Fisher, A. M. Afshar, M. S. Skolnick, D. M. Wittaker, and J. S. Roberts, Phys. Rev. B **53**, 10 469 (1996).

[9] T. Tanaka, Z. Zhang, M. Nishioka, and Y. Arakawa, Appl. Phys. Lett. **69**, 887 (1996).

[10] J. D. Berger, O. Lyngnes, H. M. Gibbs, G. Khitrova, T. R. Nelson, E. K. Lindmark, A. V. Kavokin, M. A. Kaliteevsli, and V. V. Zapasskii, Phys. Rev. B **54**, 1975 (1996).

[11] J. Tignon, P. Voisin, C. Delalande, M. Voos, R. Houdré, U. Oesterle, and R. P. Stanley, Solid-State Electron. **40**, 497 (1996).

[12] E. D. Jones, S. K. Lyo, I. J. Fritz, J. F. Klem, J. E. Shirber, C. P. Tigges, and T. J. Drummond, Appl. Phys. Lett. **54**, 2227 (1989).

[13] R. L. Greene and K. K. Bajaj, Phys. Rev. B **31**, 6498 (1985).

[14] A. H. MacDonald and D. S. Ritchie, Phys. Rev. B **33**, 8336 (1986).

[15] S. R. Eric Yang and L. Sham, Phys. Rev. Lett. **24**, 2598 (1987); and also G. E. W. Bauer and T. Ando, Phys. Rev. B **37**, 3130 (1988).

[16] G. Bastard, *Wave Mechanics Applied to Semiconductor Heterostructures* (Les Editions de Physique, Les Ulis, 1988).

[17] Y. Zhu, D. J. Gauthier, S. E. Morin, Q. Wu, H. J. Carmichel, and T. W. Mossberg, Phys. Rev. Lett. **64**, 2499 (1990).

[18] R. Houdré, R. P. Stanley, and M. Ilegems, Phys. Rev. A **53**, 2711 (1996).

[19] D. M. Whittaker, P. Kinsler, T. A. Fisher, M. S. Skolnick, A. Armitage, A. M. Afshart, and J. S. Roberts, Phys. Rev. Lett. **77**, 4792 (1996).